

Quantifying erosion in a pre-Alpine catchment at high resolution with concentrations of cosmogenic ^{10}Be , ^{26}Al , and ^{14}C

Chantal Schmidt^{1,2}, David Mair¹, Naki Akçar¹, Marcus Christl³, Negar Haghpor³, Christof Vockenhuber³, Philip Gautschi³, Brian McArdell², Fritz Schlunegger¹

¹ Institute of Geology, University of Bern, Bern, 3012, Switzerland

² Swiss Federal Research Institute WSL, Birmensdorf, 8903, Switzerland

³ Laboratory of Ion Beam Physics, ETH Zurich, Zürich, 8093, Switzerland

10 *Correspondence to:* Chantal Schmidt (chantal.schmidt@unibe.ch)

Abstract

Quantifying erosion across spatial and temporal scales is essential for assessing different controlling mechanisms and their contribution to long-term sediment production. However, the episodic supply of material through landsliding complicates quantifying the impact of the individual erosional mechanisms at the catchment scale. To address this, we combine the results of geomorphic mapping with measurements of cosmogenic ^{10}Be , ^{26}Al , and ^{14}C concentrations in detrital quartz. The sediments were collected in a dense network of nested sub-catchments within the 12 km²-large Gürbe basin that is situated at the northern margin of the Central European Alps of Switzerland. The goal is to quantify the denudation rates, disentangle the contributions of the different erosional mechanisms (landsliding versus overland flow erosion) to the sedimentary budget of the study basin, and to trace the sedimentary material from source to sink. In the Gürbe basin, spatial erosion patterns derived from ^{10}Be and ^{26}Al concentrations indicate two distinct zones: [the](#) headwater zone with moderately steep hillslopes dominated by overland flow erosion, with high nuclide concentrations and low denudation rates (~ 0.1 mm/yr), and [a](#) steeper lower zone shaped by deep-seated landslides, ~~where~~. [Here](#) lower concentrations correspond to higher denudation rates (up to 0.3 mm/yr). In addition, $^{26}\text{Al}/^{10}\text{Be}$ ratios in the upper zone align with the surface production ratio of these isotopes (6.75), which is consistent with sediment production through overland flow erosion. In the lower zone, higher $^{26}\text{Al}/^{10}\text{Be}$ ratios of up to 8.8 point towards sediment contribution from greater depths, which characterises the landslide signal. The presence of a knickzone in the river channel at the border between the two zones points to the occurrence of a headward migrating erosional front and supports the interpretation that the basin is undergoing a long-term transient response to post-glacial topographic changes. In this context, erosion rates inferred from ^{10}Be and ^{26}Al isotopes are consistent, suggesting a near-steady, possibly self-organised sediment production regime over the past several thousand years. ~~In such a regime, individual and stochastically operating landslides are aggregate over time result in a specific region~~ [the generation of higher erosion with an aggregated signal that is recorded as a higher average denudation rate by the cosmogenic isotopes.](#) Although in-situ ^{14}C measurements were also conducted, the resulting concentrations ~~show a non-conclusive~~ [are difficult to interpret as soil mixing \(due to landsliding\), sediment storage or an increase in erosion rates might influence the \$^{14}\text{C}\$ concentration pattern in a yet non-predictable way.](#)

35 1 Introduction

In alpine environments stochastic processes such as landslides often drive sediment production and condition the occurrence of debris flows (Kober et al., 2012; Clapuyt et al., 2019). During periods of strong hillslope-channel coupling, the processes operating on the hillslopes deliver detrital material to the channel network, where sediment from various sources becomes mixed and transported downstream. As a consequence, the sediments at the outlet of ~~an alpine~~ such a catchment are a mixture
40 of detrital material generated through a large variety of erosional mechanisms in different locations in the upstream basin. This makes it challenging to allocate the detrital material and to quantify how the different sub-catchments and erosional processes have contributed to the overall sediment budget. (Battista et al., 2020). This is particularly the case for those basins that are underlain by a homogenous bedrock lithology, which prevents the identification of different sediment sources using petrologic fingerprinting methods (e.g., Stutenbecker et al., 2018). In such a context, in-situ ^{10}Be has proven a useful tool to quantify the
45 generation of sediment through erosion (Bierman and Steig, 1996; vonBlanckenburg, 2005) across a large range of catchment sizes – from small headwater basins ($\sim 1 \text{ km}^2$; Granger et al., 1996) to major river systems such as the Ganges and Amazon rivers (Wittmann et al., 2009; Dingle et al., 2018). In addition, ^{10}Be -derived denudation rates have also been successfully applied to explore the controls of various parameters on surface erosion such as: topography, ~~and~~ rock strength (DiBiase et al., 2010; Carr et al., 2023), ~~environmental conditions (Reber et al., 2017; Starke et al., 2020), rock uplift as well as climatic~~
50 ~~variables including precipitation (Roda-Boluda et al., 2019; Chittenden et al., 2014),~~ ~~environmental conditions (Reber et al., 2017), rock uplift as well as climatic variables including precipitation (Roda-Boluda et al., 2019),~~ runoff and runoff variability (Savi et al., 2015), ~~and frost cracking processes (Delunel et al., 2010; Savi et al., 2015)~~. However, a successful ^{10}Be -based assessment of basin-averaged denudation rates requires that the material at the sampling site is well mixed (Binnie et al., 2006), representing the contributions from the various tributary basins according to the rates at which sediment has been generated in
55 them. In catchments where sediment has been episodically supplied e.g., by landslides, denudation rate estimates may be biased towards the impact of a specific sediment source (~~Bierman and Steig, 1996; Savi et al., 2014~~)(Bierman and Steig, 1996; Savi et al., 2014; Brardinoni et al., 2020), particularly if samples are collected in small basins (Yanites et al., 2009; Marc et al., 2019). Accordingly, erosion rate estimates for basins where the sediment production has largely been controlled by landslides requires a sampling strategy where the corresponding upstream size of the basin increases with landslide area if the
60 goal is to capture a stable long-term erosion rate signal (Niemi et al., 2005; West et al., 2014). This is also the main reason why few studies have targeted small catchments with stochastic sediment delivery (Niemi et al., 2005; Kober et al., 2012). Nonetheless, recent work (DiBiase, 2018) has demonstrated that landslides primarily introduce some scatter, but not a strong bias into erosion rate estimates. Furthermore, the use of paired cosmogenic isotopes with different half-lives, such as ^{10}Be – ^{26}Al (Wittmann and von Blanckenburg, 2009; Hippe et al., 2012; Wittmann et al., 2011) or ^{10}Be – ^{14}C (Slosson et al., 2022; Skov et al., 2019; Hippe et al., 2019; Kober et al., 2012) have enabled to reconstruct the occurrence of sediment storage in the
65 source-to-sink sedimentary cascade. They also improved our understanding about the importance of transient erosional effects on the generation of the cosmogenic signals in fluvial material (e.g., Hippe et al., 2012).

Here, we use information offered by concentrations of cosmogenic ^{10}Be , ^{26}Al , and ^{14}C in riverine quartz, which we combine with the results of geomorphic mapping. The goal is to (i) trace the origin of the sediments, (ii) document the influence of landsliding on the long-term sediment fluxes, and to (iii) explore the scale-dependency – in space and time – of the resulting cosmogenic signals. In contrast to most previous studies, we particularly target small basins to identify the impact of landslides on the generation of cosmogenic signals. To this end, we focus our work on the Gürbe basin situated at the northern margin of the European Alps. Erosion in this basin has been largely controlled by a large variety of erosional processes including sediment supply through deep-seated landslides (do Prado et al., 2024), thus making this basin an ideal target for our goals. We thus ~~conduct a dense sampling program in this catchment and combine~~ address our aims using the ~~results~~ concentrations of the three cosmogenic isotopes (^{10}Be , ^{26}Al , and ^{14}C) ~~to allocate in quartz minerals, which we extracted from detrital sediments in the origin channel network of the material, quantify the scaling – both in space and time – of the erosional processes operating in the study~~ Gürbe basin, ~~and to trace the elastic material from the source to the sink.~~

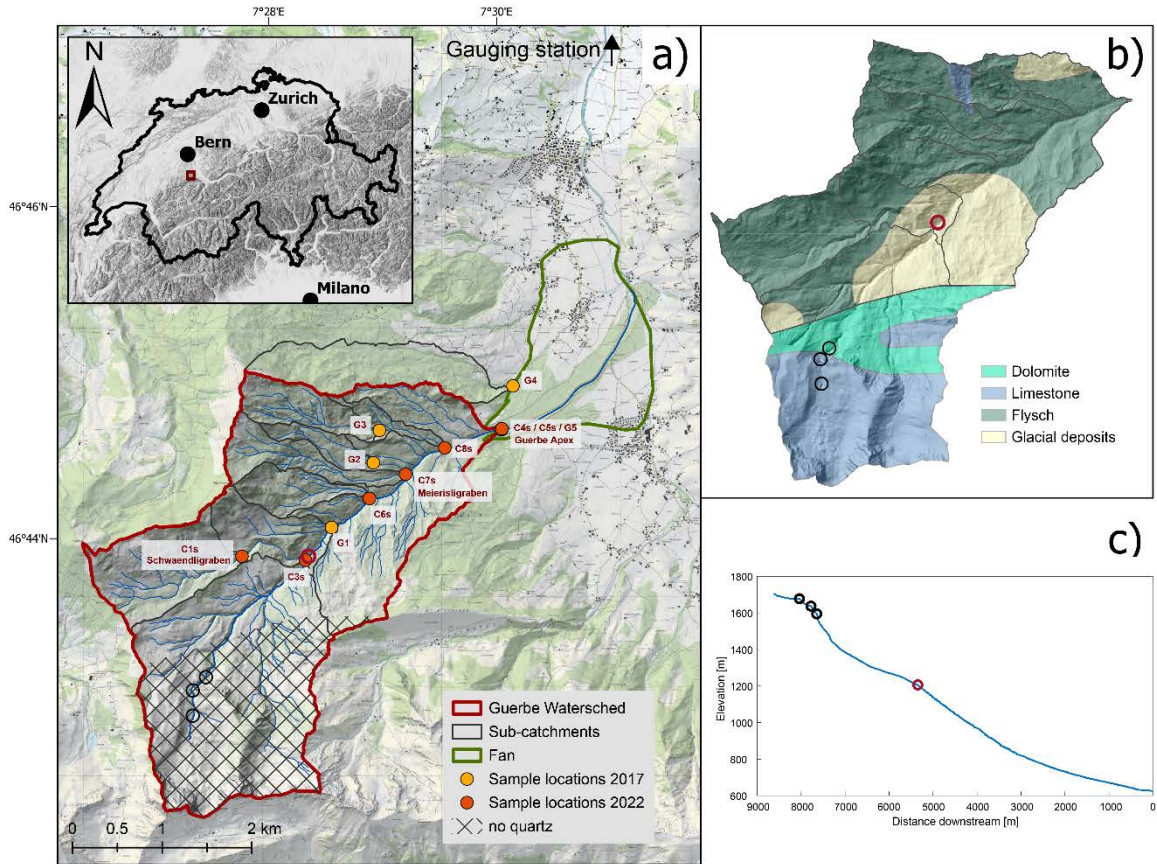
2 Local setting

The study area, the 12 km^2 -~~large~~ Gürbe catchment, is situated at the northern margin of the Swiss Alps (Fig. 1a). The Gürbe River, with a ~~~8 km-long~~ main channel ~~approximately 8 km long~~, originates at an elevation of approximately 1800 m a.s.l. There the landscape is characterised by steep cliffs ~~made up~~ of Mesozoic limestones that are part of the Penninic Klippen belt (Jäckle, 2013) (Fig.-1b). These units are partially covered by a several-~~meter-thick~~ layer of glacial deposits (i.e. till, Swisstopo, 2024a). The orientation of the corresponding moraine ridges suggest deposition by small, local glaciers during the Last Glacial Maximum (LGM) ca. 20'000 years ago (Bini et al., 2009; Ivy-Ochs et al., 2022). The headwater area of the Gürbe catchment hosts a second main tributary, the Schwändligraben River (Fig. 1a), ~~which~~. ~~It~~ originates within Cretaceous to Eocene Gurnigel-Flysch units ~~comprised of alternating layers, which are alternations~~ of marls, sandstones, polymictic conglomerates and mudstones (Winkler, 1984). The landscape in the source area of this tributary is characterised by a swampy terrain and ancient deep-seated gravitational slope failures. At approximately 1200 m a.s.l., a knickzone that corresponds to the highest glacial deposits of the LGM Aare-glacier in this region (Bini et al., 2009) separates the landscape ~~into~~ an upper and a lower zone. At this knickzone, the longitudinal profile of the Gürbe River steepens from originally 6.5° ~~upstream of this knickzone~~ to 9.3° ~~farther downstream~~ (Fig. 1c). Similarly to the region upstream of the knickzone, the bedrock in the lower part of the Gürbe basin is predominantly composed ~~of alternated sandstones and mudstones~~ ~~mudstone beds~~ that either occur in the Gurnigel-Flysch unit (Swisstopo, 2024a) or in the Lower Marine Molasse (Diem, 1986). In this lower part of the Gürbe basin, the hillslopes are between 20° and 25° steep and covered by a dense forest made up of spruce. ~~Five~~ Several areas prone for ~~landsliding~~ the occurrence of deep-seated landslides have been identified in the lower part of the Gürbe basin, ~~where three of them are located on the SE side and two on the NW side of the valley~~ (Zimmermann et al., 2016). ~~These landslides are known for their re-current activities during the past decades either experiencing a slow, continuous movement or periodic reactivations. The dynamics of these landslides are characterised by short episodes of accelerated slip~~

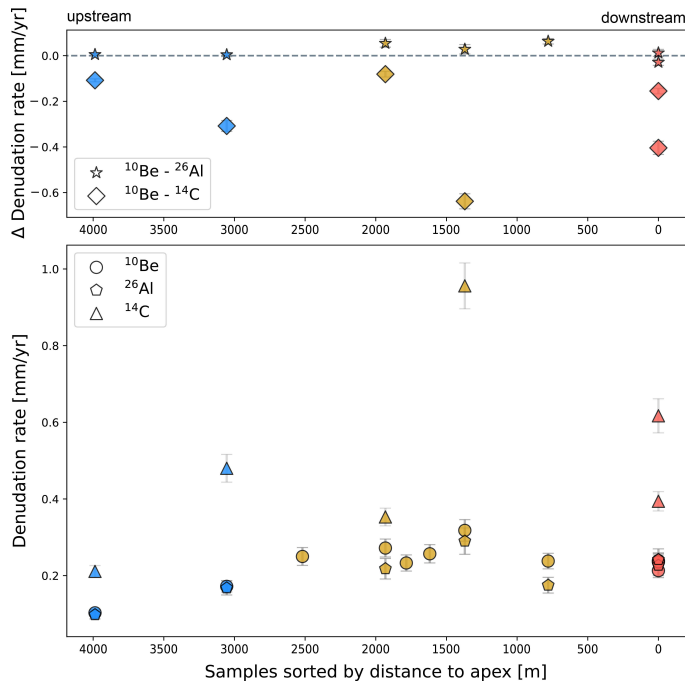
100 in the range of several meters to tens of meters per day, followed by period during which the landslides have been stable
(Zimmermann et al., 2016). In locations where the toes of the deep seated landslides reach the Gürbe channel, the surfaces of
these hillslope failures are reworked by secondary shallow seated landslides, marking fresh scars in the topography. Also, in
this lower part of the catchment, the Gürbe River has been actively incising into bedrock, thereby re-activating most of these
105 of the Gürbe basin (Salvisberg, 2017). Most of them have been inactive for several tens of years (Zimmermann et al., 2016).
During these times, sediment has mainly been generated through a combination of overland flow erosion and incision by small
torrents that are perched on these landslides. Yet, all of these landslides have also been re-activated periodically, though not
simultaneously. During such periods lasting several days up to several months, they have experienced high slip rates of several
meters per day (Zimmermann et al., 2016). This has resulted in a major re-mobilization of mass also during the following years
110 when the landslides have become inactive. Notably, most of the active landslides are not directly connected to the main Gürbe
channel (Figs. 2, 3d, e). Therefore, the delivery of material from these landslides to the trunk stream occurred primarily via
lateral tributaries. In cases where such deep-seated mass movements do reach the Gürbe River, undercutting by fluvial
processes has triggered secondary shallow-seated landslides at their toes, resulting in material from the large landslides being
directly supplied to the trunk stream. The combined effect of the aforementioned processes is a relatively high mean annual
115 sediment discharge of c. 900 – 2600 m³/a at the downstream end of the Gürbe basin (Zimmermann et al., 2016; do Prado et
al., 2024). This was the main reason why approximately 140 check dams have been built during the past century to stabilise
the streambed, reduce the gradient, and thereby regulate the transport of bedload (Salvisberg, 2017; do Prado et al., 2024). At
the downstream end of the lower section, the Gürbe channel transitions into the deposition zone, forming an approximately 4
km² alluvial fan with a distinct apex situated at 800 m a.s.l. On this fan and farther downstream, the Gürbe River flows in an
120 artificial channel that is stabilised by check dams and flood protection dikes. After passing through an artificial deposition
area, the river enters the Gürbe valley floodplain, where the stream flows in a confined channel until merging with the Aare
River approximately 20 km downstream.

The runoff conditions of the Gürbe River are characteristic for a pre-alpine environment, exhibiting a nivo-pluvial discharge
regime (Salvisberg, 2017; Jäckle, 2013). Between 1981 to 2010 the discharge of the Gürbe River has been continuously
125 measured at the Burgistein gauging station that is situated ca. 5 km downstream of the Gröbe fan (Fig. 1a). During this period,
the mean annual precipitation rates have ranged from approximately 1100 mm/year in the alluvial fan area to nearly 2000
mm/year in the headwaters of the catchment (Frei et al., 2018; based on MeteoSwiss, 2014). Due to the low water storage
capacity of the soils, including the soils in the Peninic Klippen Belt and the regolith cover of the highly saturated, low-
permeability Gurnigel Flysch and Lower Marine Molasse units, the catchment rapidly responds to high rainfall rates, resulting
130 in peak floods with short durations (Ramirez et al., 2022). The gauging records indeed show that intense summer
thunderstorms, with rainfall intensities up to 30 mm/h, tend to generate large discharge events. The highest recorded water
discharge of 84 m³/s occurred on the 29th of July 1990, (Ramirez et al., 2022; do Prado et al., 2024) runoff with large discharge
magnitudes. Such an event with an extremely high discharge of 84 m³/s occurred on the 29th of July 1990 (Ramirez et al.,

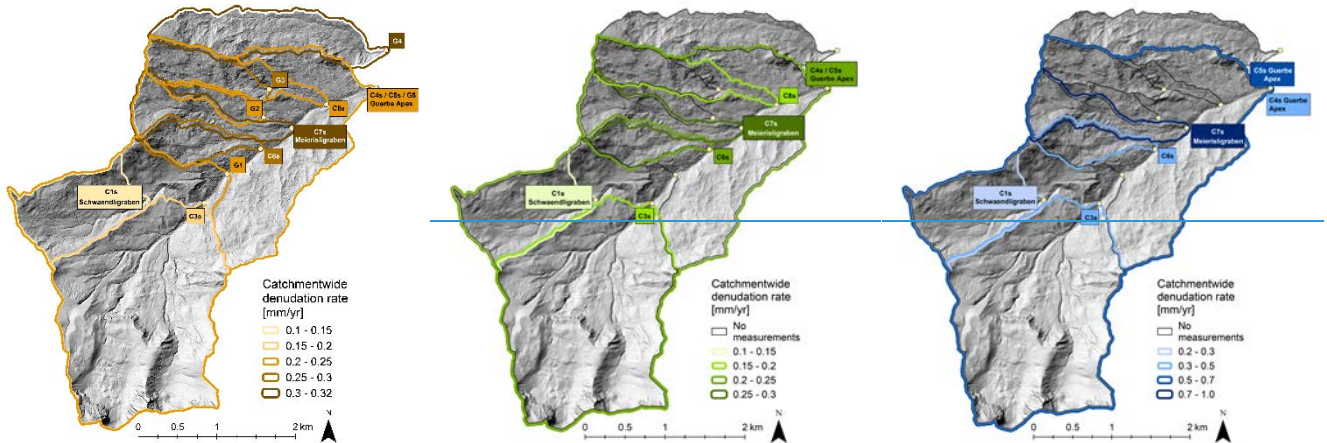
135 [SuchThese](#) [2022; do Prado et al., 2024](#)). In contrast, the mean annual discharge has been approximately 1.3 m³/s during the survey period. [These](#) high discharge variabilities emphasise the torrential character of the Gürbe River (Ramirez et al., 2022; Salvisberg, 2022).



the minimum duration of exposure required to accumulate the measured ^{10}Be and ^{26}Al concentrations ranges from 2'000 to 6'000 years, while for ^{14}C concentrations it ranges from 800 to 3'000 years- (Table S6).



420 **Figure 34:** Denudation rates calculated based on the measured ^{10}Be , ^{26}Al and ^{14}C concentrations. Each colour indicates the zone represented by the sample represents corresponding samples, with blue characterizing the upper zone, yellow the lower zone, and red the Gürbe fan apex. DigitalThe digital elevation model (DEM) is taken from the Federal Office of Topography swisstopo (Swisstopo, 2024d).



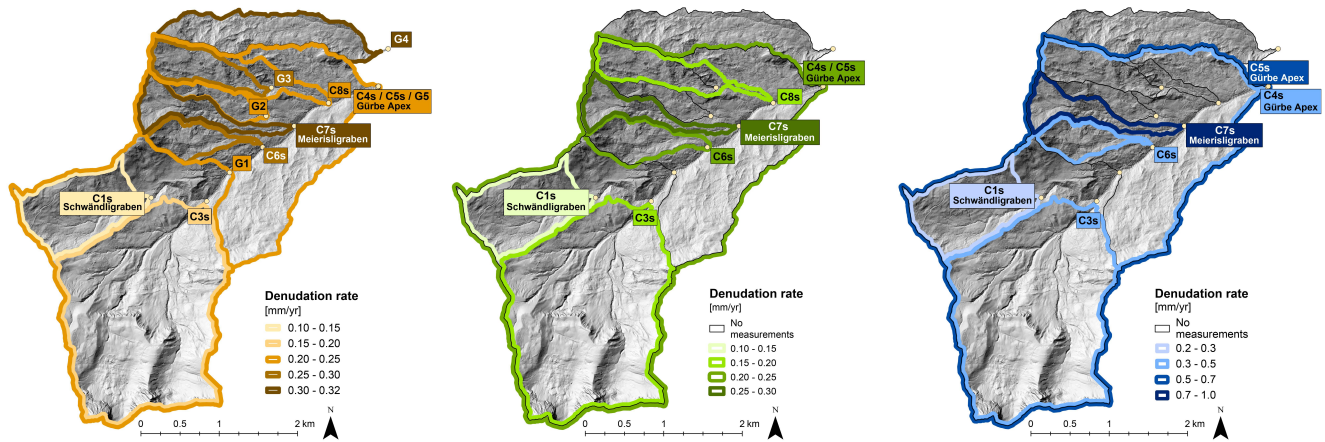


Figure 4: Calculated denudation rates based on the ^{10}Be (left), ^{26}Al (middle) and ^{14}C (right) concentrations. The lighter colours illustrate the highest concentrations (measured in the sample C1s representing the Schwändligraben sub-catchment in the upper zone). The lowest nuclide concentrations were measured in the sample C7s, representing the Meierisligraben tributary in the lower zone. The digital elevation model (DEM) is taken from the Federal Office of Topography swisstopo (Swisstopo, 2024d).

4.4 Geochemical sediment composition of sediment

The analysed samples showed variable SiO_2 content (33 -58 %-wt) and Al_2O_3 (5 – 12 %-wt), which are anticorrelated with CaO concentrations (8% to 29%; Table S6). Here, the samples from catchments with limestone-bearing bedrock lithologies (e.g. C3s; Fig. 2) show the highest concentrations of CaO and the lowest ones of SiO_2 and Al_2O_3 (Table S6), leading to resulting in a downstream decrease of pattern where the CaO concentrations with a downstream decreasing decrease in the downstream direction. This reflects the corresponding trend in exposed lithologies where the relative proportion of limestone lithologies. All limestones in the basin decreases downstream. The relative abundance of all other major oxides did vary significantly between individual samples (Table S6). Similarly, the concentrations of the trace elements did not vary strongly, with the main trace elements being Sr (325 ppm to 717 ppm), Ba (140 ppm to 310 ppm) and Zr (90 ppm to 220 ppm). Aside from the downstream-decreasing trend of geochemical signals associated with limestone content in favour lithologies (Penninic Klippen Belt) – relative to those indicative of SiO_2 - SiO_2 - and Al_2O_3 - Al_2O_3 -rich litharenites, bedrock (Flysch and Molasse units) – no systematic variation in geochemical composition is visible in both observed, either for the major oxides and measured or for the trace elements (Supplementary Fig. S1).

5 Discussion

The concentrations of the cosmogenic isotopes ^{10}Be and ^{26}Al and the resulting erosion rates show distinct differences between the upper, gently sloping region and the lower, steeper zone of the catchment (Figs. 34 and 45). We first discuss the implications of this pattern and particularly explore how the cosmogenic signals within the Gürbe basin change in the downstream direction as sediments derived from landslides impact the cosmogenic signal towards the catchment's outlet near the fan apex (section 5.1). Next, we combine the ^{10}Be , ^{26}Al , and ^{14}C datasets to investigate the erosional dynamics across different temporal scales. By comparing the signals preserved by these isotopes, we assess whether the cosmogenic nuclide concentrations reflect the occurrence of steady erosion over varying timescales, or if they record the effects of inheritance, burial, or transient perturbations over the same timescales (sections 5.2 and 5.3). As a next aspect, we discuss (i) how the cosmogenic nuclide-based erosion rates relate to the landscape's architecture by comparing them with the mapping results (section 5.4), and (ii) how this pattern has been conditioned by the glacial carving during the past glaciations (section 5.5). We end the discussion with a notion that in drainage basins where the bedrock is too homogeneous to pinpoint the origin of the detrital material, terrestrial cosmogenic nuclides offer a viable tool for provenance tracing (section 5.6).

5.1 Downstream propagation and scale dependency of cosmogenic signals

The ^{10}Be and ^{26}Al concentrations, and consequently the inferred denudation rates, record the occurrence of a variety of erosional mechanisms across the Gürbe basin. In the upper part of the catchment, high cosmogenic nuclide concentrations correspond to low denudation rates. This contrasts with the lower nuclide concentrations and higher erosion rates inferred for the samples collected in the tributaries of the lower zone, [along the incised reach downstream of the knickzone \(sample G1\)](#), and at the fan apex (Fig. 56). This downstream decrease in concentrations of both nuclides suggests that the pattern of sediment generation has been stable over the erosional timescale recorded by them. Such an interpretation is corroborated by the same nuclide concentrations (within uncertainties) encountered in the three riverine samples at the fan apex. This is surprising because sediment supply through landsliding – in our case in the lower zone – introduces a stochastic variability into the generation of sediment. Such a mechanism was already demonstrated for other Alpine torrents (Kober et al., 2012; Savi et al., 2014), where stochastic processes such as landslides and debris flows have resulted in episodic supply of sediment with low ^{10}Be concentrations (Niemi et al., 2005; Kober et al., 2012). This has the potential to perturb the overall cosmogenic signal particularly in small catchments (Yanites et al., 2009; Marc et al., 2019), thereby (i) leading to variations in nuclide concentrations within riverine sediments collected from the same channel bed (Binnie et al., 2006) and (ii) introducing scatter into the dataset (DiBiase et al., 2023). Given the small area (12 km²) and the prevalence of recurrent landslides in the Gürbe sub-catchments, one might expect the sedimentary material at the Gürbe fan apex to record such variations. Yet our results indicate that the overall denudation signal has remained nearly stable at the fan apex (Fig. 56). This highlights an important scale-dependency in the erosional controls governing the generation of cosmogenic signals in the Gürbe basin. In particular, at smaller spatial scales (0.25 – 3.5 km²), denudation rates reflect the controls of local geomorphic and geologic conditions on

erosion and material supply, such as repeated deep-seated landsliding as in the case presented here. However, when these signals with a local origin are aggregated downstream towards the fan apex, they are recorded as a mixed, more stable signal that averages out the high and low concentrations generated in the individual sub-catchments. In the Gürbe basin, such mixing appears to occur at a spatial scale of less than 10 km². We thus infer – as this has already been mentioned by the many studies referred to in this paper in previous sections – that cosmogenic nuclides remain a suitable tool for estimating long-term average erosion rates over thousands of years for landscapes eroding with rates between 0.1 and <1 mm yr⁻² (vonBlanckenburg, 2005). This holds true even in that have been eroded at rates between 0.1 and <1 mm/yr (von Blanckenburg, 2005). This holds true even for catchments influenced by repeated stochastic processes – such as those documented for landslide processes in the Gürbe basin – provided that the sediment is sufficiently well mixed and that the corresponding cosmogenic nuclides are in an isotopic steady state (Clapuyt et al., 2019).

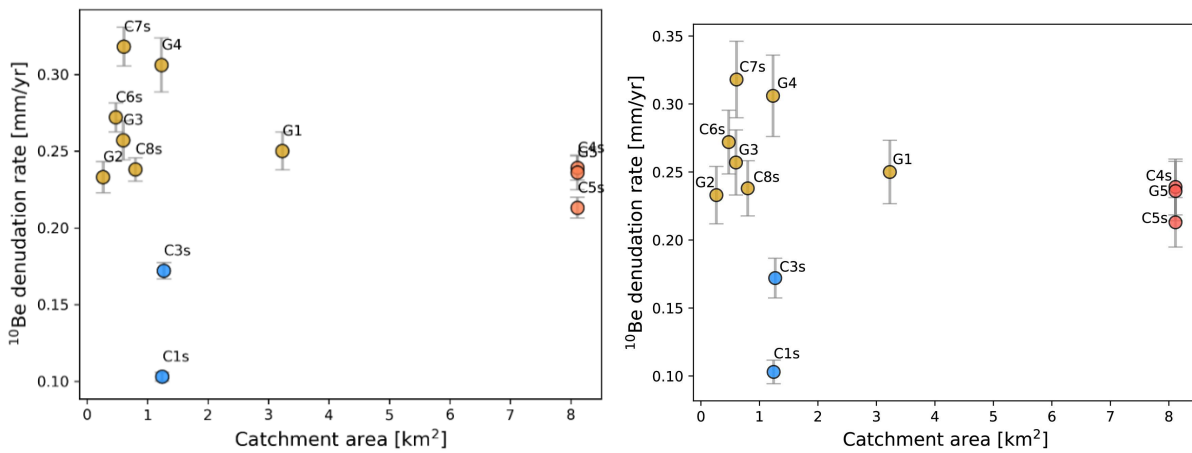


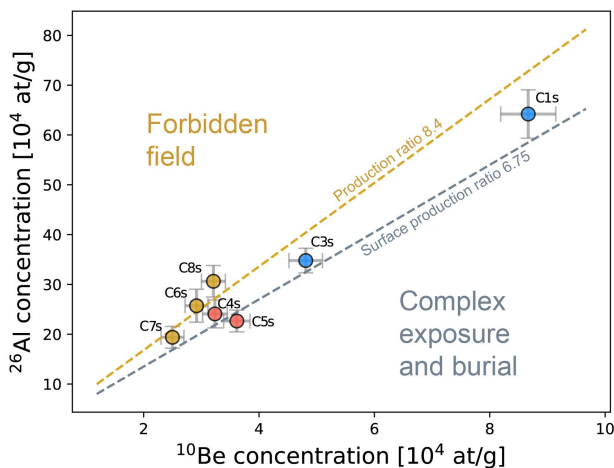
Figure 56: Scale dependency of erosion rate estimates with concentrations of in-situ ¹⁰Be. The variety of erosion rates determined for the scales of small local catchments (blue for the upper zone and yellow for the lower zone) is averaged out for the samples collected at the fan apex (red) where concentrations of in-situ ¹⁰Be characterise the mixed erosional signal of the entire catchment and thus for a larger scale.

5.2 Steadiness of the denudation signals across time scales

Concentrations of cosmogenic nuclides in riverine quartz have the potential to record the erosional history of a landscape, provided that (i) the nuclide production has occurred at a steady rate across the spatio-temporal scale over which they integrate erosion rates, and (ii) the nuclides are saturated (e.g., vonBlanckenburg, 2005). A potential deviation from these assumptions could be caused by a sedimentary legacy from past glaciations (Jautzy et al., 2024). This also concerns the Gürbe basin, as the study area has a history of erosion and material deposition by local and regional glaciers – most notably by the Aare glacier. The coverage of the surface by glaciers could have led to transient shielding of the surface during glacial times, potentially distorting the cosmogenic isotope signal (Slosson et al., 2022). Yet our ¹⁰Be and ²⁶Al-based denudation rates point to an integration time < 8,000 years, whereas for ¹⁴C, it is even shorter with < 3,000 years (Table S6). These ages are significantly

younger than the last major glacial advance at around 12-11 ka ago (Ivy-Ochs et al., 2009). Therefore, we conclude that a [potential](#) inheritance from pre-glacial surfaces does not significantly affect our data for all nuclides.

500 A further potential bias in quantifying denudation rates with cosmogenic nuclides could be introduced through sediment storage and reworking along the sediment cascade (e.g., Wittmann et al., 2020; Halsted et al., 2024). However, the ratios of the ^{10}Be and ^{26}Al concentrations are close to the values characterizing a nuclide production close to the surface (Fig. 67). Additionally, the resulting denudation rates are overall in good agreement with each other, at least in the upper zone and at the basin's outlet. This suggests that the ^{10}Be and ^{26}Al concentrations do not record the occurrence of a significant erosional transience during the past [kyrsmillennia](#), at least if the nuclide concentrations in the samples from the upper zone and the
505 downstream end of the Gürbe basin are considered. We therefore consider, and this has already been noted in the previous section, that the signals preserved by the concentrations of in-situ ^{10}Be and ^{26}Al do record a pattern of erosion and sediment generation that has been stable at least during the erosional timescale of both isotopes, which are several thousand years. We acknowledge, that in the lower zone the supply of material through landsliding does result in a measurable discrepancy between the ^{10}Be and ^{26}Al -based denudation rates (Figs. 3, 54, 6 and 67), a pattern which is discussed in section 5.4. We also note that
510 the denudation rate pattern of the short-lived ^{14}C is distinctly different from that of ^{10}Be and ^{26}Al , which renders interpretations thereof more complex (see next section 5.3).



515 **Figure 67:** Two-nuclide diagram showing the ^{10}Be concentrations versus the ^{26}Al concentrations. The ^{26}Al concentration is plotted against the ^{10}Be concentration. The concentrations are within the field that is characteristic for a [surface nuclide](#) production [on the surface](#). The occurrence of long-term burial can be excluded for our samples.

5.3 Potential controls on the pattern of cosmogenic ^{14}C

~~[14C-based denudation rates have been shown to be sensitive to short term perturbations \(Hippe, 2017\), particularly in landscapes dominated by stochastic processes such as debris flows and landslides \(e.g., Kober et al., 2012\), or by storage of a significant volume of sediment \(Hippe et al., 2012\). However, we present three arguments why we are not capable of disclosing](#)~~
520

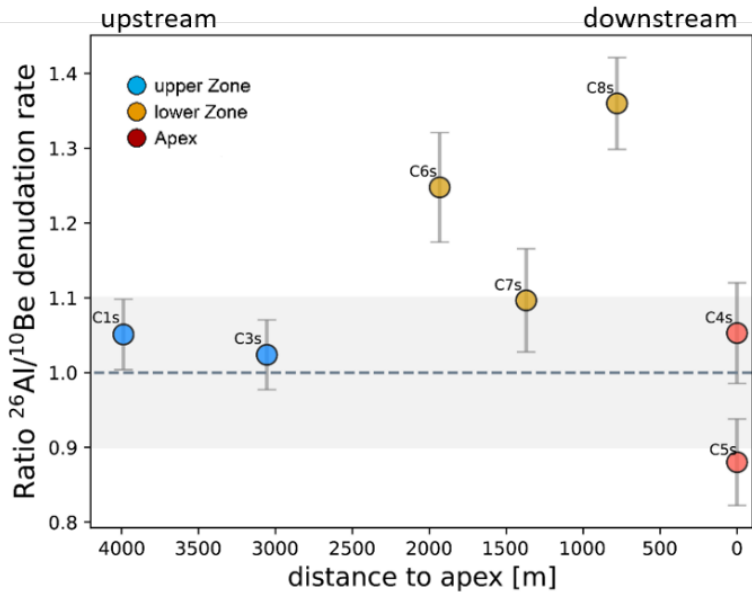
~~such controls on the ^{14}C denudation pattern in our dataset. Here, we present several arguments as to why the pattern of ^{14}C concentrations in the riverine sediments of the Gürbe basin is not straightforward to explain.~~ First, as outlined by Hippe (2017), in cases where the signal integration timespan exceeds the half-life of the corresponding cosmogenic isotope, a portion of the accumulated radionuclides will decay before the material is completely eroded. The result is a reduction of the ^{14}C concentrations, which could lead to an artificially high erosion rate (Hippe, 2017). In our case, the minimum exposure time required to accumulate the observed ^{14}C concentrations is less than 3,000 years – well below the isotope’s half-life of 5,730 years. This makes unaccounted radioactive decay an unlikely primary cause of the low ^{14}C concentrations in our samples. Second, a recent ~~increase~~change in erosion rates on timescales shorter than the signal integration-time of ^{10}Be and ^{26}Al could explain why the ^{14}C -based denudation rates are up to three times higher than the estimates derived from the other isotopes. This ~~is equivalent to~~would require a ~~situations~~scenario where the ^{14}C signal is already recording this increase in denudation, while the concentrations of ^{10}Be and ^{26}Al have not yet registered such a change. ~~While this could account for why all ^{14}C -based denudation rates are higher than those derived from the other two nuclides~~However, in rapidly eroding landscapes (> 500 mm/kyr) ^{10}Be concentrations initially adjust more rapidly to changes in erosion rates than ^{14}C concentrations (Skov et al., 2019). This difference arises from the higher muogenic production of ^{14}C at depth, which can cause a temporary increase of ^{14}C concentrations relative to ^{10}Be in freshly exposed bedrock and detrital material during periods of accelerated erosion. As a consequence, an acceleration of erosion can only be reliably detected several thousand years after the change (Skov et al., 2019; see also Mudd, 2017). The exact duration of this latency depends on both the magnitude and timing of the perturbation that caused the change. In other words, a scenario in which a period of accelerated erosion began several thousand years ago could explain why some ^{14}C -based denudation rates are higher than those derived from the other two nuclides. Yet, it does not explain the relative differences in ^{14}C -based denudation rates between the sampled catchments (Figs. 34 and 45). Particularly, the pattern is not consistent throughout any of the three zones, and the denudation rate variation within the zones is higher than the variation between the zones (Fig. 3-4). This would require a scenario in which the increase in erosion rates was different in magnitude and timing across all sub-catchments. Therefore, the inconsistent spatial pattern, along with greater within-zone than between-zone variations, suggests that the observed changes in ^{14}C concentrations cannot be explained solely by an increase in erosion rates. Third, geomorphic processes such as soil mixing or intermittent sediment storage during transport could in part explain the observed differences between the ^{14}C and $^{10}\text{Be}/^{26}\text{Al}$ -derived denudation rates. In particular, sediment could be stored – e.g., in response to landsliding – below the production zone of ^{14}C , during which the ^{14}C inventory is partially lost due to the radioactive decay of this isotope (Hippe et al., 2012; Kober et al., 2012; Hippe, 2017; Skov et al., 2019). Such a process ~~which~~ has been referred to as transient shielding by Slosson et al. (2022). Because the $^{10}\text{Be}/^{14}\text{C}$ ratios in the Altiplano samples range between 3.6 and 15.2 – significantly higher than the surface production ratio of 0.31 – Hippe et al. (2012) interpreted the relatively low ^{14}C concentrations in the riverine sediments as a record of storage rather than surface erosion. However, since the $^{10}\text{Be}/^{14}\text{C}$ ratios of the riverine samples in the Gürbe basin range from 0.4 to 0.75 (Fig. 8) and thus do not fully fall within the complex exposure field, we consider it unlikely that the ^{14}C concentrations primarily reflect a signal of sedimentary storage. Furthermore, in the upper zone of the Gürbe basin, we exclude the occurrence

555 of widespread storage following sediment mobilization, as there is no evidence in the landscape that such processes have taken
place (e.g., the presence of large sedimentary bodies along the channels or talus cones as was reported by Slosson et al. (2022)
from their study area-). In summary, while ^{14}C has the potential to provide valuable insights into shifts in erosional dynamics,
sediment storage, and episodic mobilization of material from deeper levels (Hippe et al., 2012; Hippe, 2017), we are unable to
conclusively determine the specific processes responsible for the observed pattern of ^{14}C concentrations and denudation rates
560 in the Gürbe basin.

5.4 Landscape architecture and corresponding ^{10}Be and ^{26}Al signals

The comparison of the geomorphic map with the ^{10}Be and ^{26}Al concentrations and the calculated denudation rates exhibits a
distinct difference between the upper and lower zone, each characterised by specific topographic features and dominant
erosional processes. Specifically, the landscape in the upper zone of the Gürbe catchment is characterised by smooth slopes
565 and the occurrence of partly incised channels with low steepness values and a low connectivity to the hillslopes. Such properties
are characteristic for a landscape where overland flow erosion, ~~or~~ also referred as hillslope diffusion according to Tucker and
Slingerland (1997), have controlled the generation of clastic sedimentary material (van den Berg et al., 2012). The high
cosmogenic nuclide concentrations and, as consequence, the low denudation rates together with the $^{26}\text{Al}/^{10}\text{Be}$ concentration
ratios of 7.41 ± 0.69 and 7.23 ± 0.67 – that are close to the surface production ratio of 6.75 (Balco et al., 2008; Nishiizumi et
570 al., 1989) – are consistent with such an interpretation (Figs. ~~6 and~~ 7). The similarity in the denudation rates calculated for the
two long-lived nuclides supports the interpretation of ~~a stable undisturbed an~~ a stable undisturbed an erosional regime without significant perturbations
(Fig. 9a), at least for the time scale of thousands of years as recorded by both isotopes. We note that shallow landslides and
localised rockfall do occur in this upper zone, but the resulting deposits are partly disconnected from the channel network,
thereby minimizing their impact on the sediment budget of the Gürbe catchment (Fig. 2 & 3). In contrast, the lower zone
575 exhibits a more dynamic erosional regime, where steeper slopes (20° to 25°) together with the predominant occurrence of
mudstones in the Flysch and Upper Marine Molasse bedrock (Diem, 1986) offer ideal conditions for the displacement of
~~mid-medium-~~ to deep-seated landslides. Mapping also shows that landslides have impacted the sediment budget of the Gürbe
River either through direct material supply ~~of sediment~~ into the main channel, where ~~it~~ material is ~~then~~ subsequently remobilised
and transported downstream, or through erosion of ~~the~~ landslide bodies by ~~tributaries~~ tributary streams and associated hillslope
580 processes such as overland flow erosion and shallow-seated landslides, thereby reworking the previously displaced material.
~~The~~ In general, such stochastic ~~nature of landsliding processes~~ results in episodic sediment inputs with relatively low ^{10}Be
concentrations, as material is exhumed fast from greater depths (e.g., Niemi et al., 2005). ~~We use these mechanisms to explain~~
~~the relatively high~~ $^{26}\text{Al}/^{10}\text{Be}$ ~~ratios between~~ 7.76 ± 1.07 ~~to~~ 9.54 ± 1.17 (Fig.). ~~In the Gürbe basin, however, most landslides~~
~~have remained dormant for decades, but have regularly been re-activated with slip rates of several meters per day. These re-~~
585 ~~activations have resulted in the excavation of material along multiple trajectories from depth to the surface, and finally to the~~
~~channel network. The mixing of material from different exposure trajectories (Fig. 9b) most likely explains the relatively high~~
 ~~$^{26}\text{Al}/^{10}\text{Be}$ concentration ratios between~~ 7.76 ± 1.07 ~~to~~ 9.54 ± 1.17 (Fig. 6) that we determined for the riverine material in three

tributaries with material sources in these landslides. Additionally, the discrepancy between the ^{10}Be - and ^{26}Al -based erosion rates – with ratios ranging from 1.1 to 1.4 (Fig. 7) – suggests is a further support of the inferred complex erosional history involving material sourced from varying depths and subjected to different pathways during transport along the sediment cascade (Fig. 9a). These findings reinforce the view wheredemonstrate that the occurrence of landsliding not only results in an overall increase of erosion rates but also introduces a variability in the cosmogenic nuclide signals as seen here by the $^{26}\text{Al}/^{10}\text{Be}$ concentration ratios. Yet, if such cycles of landslide quiescence and activity have occurred multiple times and at different locations in a basin, the resulting cosmogenic concentrations will converge to a stable cosmogenic signal farther downstream and thus for a large spatial scale. This is the case for the outlet of the Gürbe basin where we determine consistent cosmogenic nuclide signals. This implies that at the scale of individual tributary basins, which is $< 2 \text{ km}^2$ in our case, the production of sediment can be highly stochastic. At the scale of an entire basin – in our case the Gürbe basin with a size of 8 km^2 – the ensemble of the stochastic processes converges to a sediment cascade that can be characterized as steady state, at least for the time scale recorded by the cosmogenic isotopes.



600

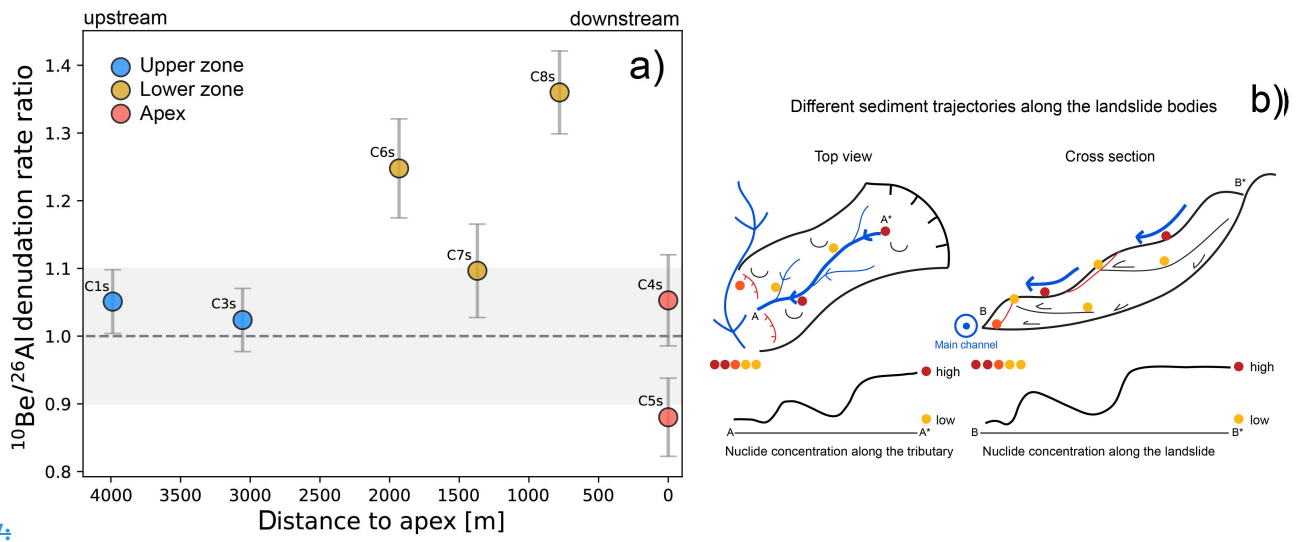


Figure 7:

Figure 9: Sediment cascade in the Gürbe basin recorded by cosmogenic nuclides (a) Ratios between ^{26}Al - and ^{10}Be -based denudation rates. In the upper zone the ratios between the denudation rate calculated with both isotopes are in very good agreement. In the lower zone the ^{26}Al -based denudation rates are lower than the ^{10}Be -based rate, leading to ratios that are larger than one. At the fan apex the ratios between both rates are in a relatively good agreement. The grey shading is representing the $\pm 10\%$ envelope of the isotope ratio. (b) conceptual model of different sediment trajectories along the medium- to deep-seated landslide bodies leading to lower nuclide concentrations in tributaries.

5.5 The importance of glacial conditioning as an erosional driving force

In a previous study, Delunel et al. (2020) showed that a large part of the catchment-averaged denudation rates in the European Alps can be understood as a diffusion-type of process, or a mechanism referred to as overland flow erosion (e.g., Battista et al., 2020) where denudation rates linearly – or a mechanism which we refer to as overland flow erosion following Battista et al. (2020) – where denudation rates increase with mean-basin hillslope angles until a threshold hillslope angle of 25° - 30° (Schlunegger and Norton, 2013). Because the hillslope angles in the Gürbe catchment are below the 25° threshold, one would predict an erosional signal that could indeed be explained by such a mechanism. While indeed all our denudation rates do fall in the predicted corresponding range of denudation rate ranges (cf. Fig. 5 of Delunel et al., 2020) and since such an assignment is certainly correct for the upper part of the Gürbe catchment (section 5.4), the lower zone challenges deviates from this simplistic acknowledgeably useful categorization. Indeed, despite the slopes being flatter than 25° , erosion in this region has been dominated by deep-seated landslides that are perched by a channel network in which the eroded landslide material has been evacuated downstream. Such a combination of processes has typically been reported for landscapes steeper than 30° in the European Alps (Delunel et al., 2020) and other mountain ranges, e.g. the San Gabriel Mountains (DiBiase et al., 2023). This difference of erosion highlights the importance of another driving force than lithology alone because Flysch bedrock also occurs in the upper zone where landslides are largely absent, but where the hillslopes are less steep. Because the elevation of the knickzone separating the upper from the lower zones corresponds to the level of the LGM Aare glacier in this region (Bini et al., 2009), it is possible that the formation of the knickzone along the Gürbe River was conditioned by glacial carving during

the LGM and possibly previous glaciations. Accordingly, the relatively flat channel and hillslope morphology in the area upstream of the knickzone could be explained by damming effects related to the presence of the Aare glacier. In contrast, the shape of the topography downstream of the knickzone was most likely conditioned by erosion along the lateral margin of the Aare glacier. Accordingly, the formation of a relatively steep flank could explain why the course of the Gürbe River is steeper than would be expected for a river with a same catchment size (do Prado et al., 2024), and why erosion on the hillslopes has been dominated by landsliding instead of overland flow erosion. Similar controls were already proposed by Norton et al. (2010) and van den Berg et al. (2012) upon explaining the occurrence of landscapes dominated by gentle hillslopes upstream of glacially conditioned knickzones and steeper hillslopes downstream of them. In such a context, a lowering of the base level after the retreat of the LGM glacier would have initiated a wave of headward erosion, with the consequence that the entire catchment is in a transient stage of landscape evolution (Abbühl et al., 2011; Vanacker et al., 2015). Accordingly, while the Gurnigel Flysch and Lower Marine Molasse bedrock seem to promote the occurrence deep-seated landslides – thus overriding the expected ~~diffusion~~overland flow-controlled behaviour typically observed in catchments with similar slopes elsewhere – a steeping of the landscape due to glacial carving needs also be considered as an additional condition accelerating erosion in the lower part of the basin.

5.6 Geochemical composition of the detrital material, and the use of cosmogenic isotopes for provenance tracing with concentrations of cosmogenic nuclides

~~This study demonstrates that concentrations of cosmogenic isotopes offer suitable information for allocating the source of sediments in drainage basins where other provenance tracing methods, in our case whole rock geochemical compositions of the riverine material, yield non-conclusive results.~~ The whole rock geochemical analysis discloses a picture that is characteristic for a basin where limestones and litharenitessandstones are the main lithological constituents, as already demonstrated by Glaus et al. (2019) and Da Silva Guimarães et al. (2021) for other basins in the Alps. Yet, in contrast to the aforementioned studies, the results of our studyresearch did not allow a differentiation of the erosional signals derived from the various parts of the Gürbe basin, because here the only difference in composition among the samples seems to relate to the relative proportion of limestone constituents in the detrital material (section 4.4). However, the outcropping limestone units are only present locally in some of the headwater reaches (Fig. 2). This introduces a potential limitation: while our quartz-based cosmogenic nuclide measurements provide valuable erosion rate estimates, they are inherently blind to sediment generated from quartz-free lithologies, such as limestonelimestones. This raises the question of ~~whether preferential erosion in limestone rich areas could bias our cosmogenic signal, for example by diluting quartz contributions~~how well the total sediment load and the erosion rates – the latter ones inferred from the cosmogenic nuclide data – are in agreement with each other. In particular, high erosion rates in the headwater areas made up of limestones could lead to a high relative abundance of limestone grains in the Gürbe sediments farther downstream. In principle, thisThis, in turn, could lead toresult in an underestimation ~~or distortion~~ of the effective denudation rates. if such budgets are only based on cosmogenic isotopes.

660 However, in ~~the case of the~~our case, we observe only a limited contribution of the limestone lithologies to the sediment budget
of the entire Gürbe basin, ~~we~~ as we do not see any systematic variation in the geochemical composition of the detrital material.
We therefore consider this bias to be negligible for three reasons: (1) limestone units form prominent cliffs and appear more
665 resistant to erosion than surrounding lithologies, (2) no large-scale alternation of quartz-bearing and quartz-free lithologies is
observed in the field, and (3) the limestone outcrops are spatially limited and do not dominate catchment-wide ~~our~~cosmogenic-
based erosion. Consequently, the lack of a geochemical erosion signal is consistent with the observation that limestone does
not significantly contribute to the total sediment flux, supporting the representativeness of the cosmogenic nuclide-derived
erosion rates – ~~rates as representative~~ – particularly ~~when used as~~ we use them to ~~trace~~map spatial variations in erosion
670 mechanisms ~~the generation of sediment~~ across the basin. Material tracing with concentrations of in-situ isotopes works in basins
with spatially varying erosion rates and erosional mechanisms. In addition, because here ~~here~~ Additionally, and more important, the
use of paired nuclides – in our case ^{26}Al to ^{10}Be – yields conclusive information on the origin of the detrital material as
sediments derived from landslides ~~repeatedly supply sediments and thus~~ from deeper levels where the production ratio of ^{26}Al
and ^{10}Be is higher than on the surface (Akçar et al., 2017 ~~tend to have a higher ratio between the concentrations of both isotopes~~
675 than sedimentary particles generated through overland flow erosion alone (Akçar et al., 2017; Dingle et al., 2018; Knudsen et
al., 2020 ~~Knudsen et al., 2020~~)), the detrital material has a high $^{26}\text{Al}/^{10}\text{Be}$ concentration ratio. In contrast the ratio of the same
isotopes in sediments generated by overland flow erosion is lower. At the basin outlet, the detrital material reflects the
integrated effect of sediment generation by overland flow erosion, landsliding, and other processes, resulting in a cosmogenic
isotope signal whose strength depends on the relative contribution of each erosional process within. Accordingly, this study
680 demonstrates that concentrations of cosmogenic isotopes offer suitable information for allocating the source of sediments in
drainage basins where other provenance tracing methods, in our case whole-rock geochemical compositions of the ~~upstream~~
~~catchment~~ riverine material, yield non-conclusive results. Here, we demonstrate that ~~this concept~~ such approach to trace the
origin of the material holds even in a basin where the spatial contrasts in measured erosion rates are relatively low. In such
cases, a reconstruction of both the sediment sources and the associated erosional mechanisms requires a dense sampling
strategy, as implemented in this work – a need that was already emphasised by Clapuyt et al. (2019) and Battista et al. (2020).

Conclusions

This study demonstrates that cosmogenic nuclides are ideal tracers for identifying the origin of detrital material in basins with spatially varying erosion rates. They not only allow us to determine the region where most sediment has been generated, but also yield crucial information to reconstruct the mechanisms through which erosion has occurred (e.g., overland flow erosion versus landsliding), particularly when multiple isotopes are used. In the Gürbe basin, we were able to reconstruct such patterns and mechanisms using concentrations of in-situ ^{10}Be and ^{26}Al measured in riverine quartz. However, the concentrations of in-situ ^{14}C , which we also measured in the same samples, yielded non-conclusive results. Also in the Gürbe basin, we found that the erosional processes were different in the upper zone above the LGM trim line where the landscape is flat and sediment generation has been dominated by overland flow erosion, and in the region below it where the landscape is steeper and erosion has been accomplished by landsliding and fluvial incision. This points to a legacy of the current erosional mechanisms stemming from the glaciations, where carving of the valley flanks by the LGM (Late Glacial Maximum) and earlier glaciers steepened the landscape, thereby promoting erosion below the LGM margin following the glaciers' retreat. This initiated a wave of headward retreat and the formation of an erosional front separating an upper part with low erosion rates (overland flow erosion) from a lower part where erosion occurs more rapidly and has mainly been accomplished by landsliding. In the Gürbe basin, we identified this erosional front through the occurrence of a distinct knickzone in the longitudinal stream profile. This phase of headward retreat thus suggests that the Gürbe basin has been in a long-term transient state of topographic development where the current accelerated erosion and landsliding in the lower zone has been glacially conditioned. Yet despite this transient state of basin development, we find – based on the concentrations of cosmogenic ^{10}Be and ^{26}Al in the riverine material – that the pattern and rate of sediment generation has been quite stable and thus steady during the past thousands of years. This was surprising because landslides have the potential to introduce a stochasticity in the way of how erosion and sediment generation occurs. It thus appears that the transient adjustment of the Gürbe basin to post-glacial conditions has occurred in a near-steady, possibly self-organised way, resulting in sediment generation, which has occurred at nearly constant rates at least during the past thousands of years. Because cosmogenic ^{26}Al and ^{10}Be integrate erosional signals over millennia in the Gürbe basin—including periods during which environmental conditions have changed—we expect a similar pattern of sediment generation and transfer in the near future, even under the current warming climate. Consequently, [in the near future](#), the local authorities are likely to ~~be confronted with~~[face](#) the same sediment transfer mechanisms through the [basin and the](#) cascade of check dams as ~~they are~~[those occurring](#) today.

710

Author contributions

715 CS designed the study, conducted the analyses and wrote the paper with support by FS, DM and BM. NA offered scientific advise during sample collection and preparation, and during the analysis of the AMS results. MC, CV, PG supervised the AMS measurements of ^{26}Al and ^{10}Be and offered support for the interpretation of the MS data. NH performed the in-situ ^{14}C extraction and measured the ^{14}C concentrations. All authors contributed to the scientific processing and discussion of the results and to the drafting of the paper.

Competing interests

720 The authors declare that they have no conflict of interest

Data availability

All data used in this study are provided in tables or included in the Supplementary Materials. The swisstopo digital elevation models (DEMs) are publicly available.

Acknowledgements

725 We thank Julijana Gajic for training and supervising the lab work at the IFG as well as Priska Bähler for the total Al measurements. This work was funded through the Trebridge project funded by the Swiss National Science Foundation (SNSF project No 205912).

References

- 730 Abbühl, L. M., Norton, K. P., Jansen, J. D., Schlunegger, F., Aldahan, A., and Possnert, G.: Erosion rates and mechanisms of knickzone retreat inferred from 10 Be measured across strong climate gradients on the northern and central Andes Western Escarpment, *Earth Surf. Process. Landforms*, 36, 1464–1473, <https://doi.org/10.1002/esp.2164>, 2011.
- Akçar, N., Ivy-Ochs, S., Alfimov, V., Schlunegger, F., Claude, A., Reber, R., Christl, M., Vockenhuber, C., Dehnert, A., Rahn, M., and Schlüchter, C.: Isochron-burial dating of glaciofluvial deposits: First results from the Swiss Alps, *Earth Surf. Process. Landforms*, 42, 2414–2425, <https://doi.org/10.1002/esp.4201>, 2017.
- 735 Balco, G., Stone, J. O., Lifton, N. A., and Dunai, T. J.: A complete and easily accessible means of calculating surface exposure ages or erosion rates from 10Be and 26Al measurements, *Quaternary Geochronology*, 3, 174–195, <https://doi.org/10.1016/j.quageo.2007.12.001>, 2008.
- Battista, G., Schlunegger, F., Burlando, P., and Molnar, P.: Modelling localized sources of sediment in mountain catchments for provenance studies, *Earth Surf. Process. Landforms*, 45, 3475–3487, <https://doi.org/10.1002/esp.4979>, 2020.
- 740 Bierman, P. and Steig, E.: Estimating rates of denudation using cosmogenic isotope abundances in sediment, *Earth Surf. Process. Landforms*, 21, 125–139, 1996.
- Bini, A., Buonchristiani, J.-F., Couterand, S., Ellwanger, D., Felber, M., Florineth, D., Graf, H. R., Keller, O., Kelly, M., Schlüchter, C., and Schöneich, P.: Die Schweiz während des letzteiszeitlichen Maximums (LGM), <https://www.swisstopo.admin.ch/de> (last access: 6 December 2024), 2009.
- 745 Binnie, S., Pjillips, W., Summerfield, M., and Fifield, Keith Fifield, L.: Sediment mixing and basin-wide cosmogenic nuclide analysis in rapidly eroding mountainous environments, *Quaternary Geochronology*, 1, 4–14, <https://doi.org/10.1016/j.quageo.2006.06.013>, 2006.
- [Borselli, L., Cassi, P., and Torri, D.: Prolegomena to sediment and flow connectivity in the landscape: A GIS and field numerical assessment, *CATENA*, 75, 268–277, <https://doi.org/10.1016/j.catena.2008.07.006>, 2008.](https://doi.org/10.1016/j.catena.2008.07.006)
- [Brardinoni, F., Grischott, R., Kober, F., Morelli, C., and Christl, M.: Evaluating debris-flow and anthropogenic disturbance on 10 Be concentration in mountain drainage basins: implications for functional connectivity and denudation rates across time scales, *Earth Surf. Process. Landforms*, 45, 3955–3974, <https://doi.org/10.1002/esp.5012>, 2020.](https://doi.org/10.1002/esp.5012)
- 750 Bundesamt für Landestopografie swisstopo, Tarquini S., I. Isola, M. Favalli, A. Battistini, and G. Dotta: TINITALY, a digital elevation model of Italy with a 10 meters cell size (Version 1.1). Istituto Nazionale di Geofisica e Vulcanologia (INGV). <https://doi.org/10.13127/tinality/1.1>; DGM Österreich, geoland.at; DGM1, Bayerische Vermessungsverwaltung – www.geodaten.bayern.de; EU-DEM, provided under COPERNICUS by the European Union and ESA, all rights reserved; RGEAltI, Institut National de l’information géographique et forestière, données originales téléchargées sur <https://geoservices.ign.fr/rgealti#telechargement5m>, mise à jour du juillet 2023, 2023.
- 755

- 760 Cavalli, M., Trevisani, S., Comiti, F., and Marchi, L.: Geomorphometric assessment of spatial sediment connectivity in small Alpine catchments, *Geomorphology*, 188, 31–41, <https://doi.org/10.1016/j.geomorph.2012.05.007>, 2013.
- Christl, M., Vockenhuber, C., Kubik, P. W., Wacker, L., Lachner, J., Alfimov, V., and Synal, H.-A.: The ETH Zurich AMS facilities: Performance parameters and reference materials, *Nuclear Instruments and Methods in Physics Research Section B: Beam Interactions with Materials and Atoms*, 294, 29–38, <https://doi.org/10.1016/j.nimb.2012.03.004>, 2013.
- 765 [Chittenden, H., Delunel, R., Schlunegger, F., Akçar, N., and Kubik, P.: The influence of bedrock orientation on the landscape evolution, surface morphology and denudation \(10 Be\) at the Niesen, Switzerland, *Earth Surf. Process. Landforms*, 39, 1153–1166, <https://doi.org/10.1002/esp.3511>, 2014.](#)
- Clapuyt, F., Vanacker, V., Christl, M., van Oost, K., and Schlunegger, F.: Spatio-temporal dynamics of sediment transfer systems in landslide-prone Alpine catchments, *Solid Earth*, 10, 1489–1503, <https://doi.org/10.5194/se-10-1489-2019>,
770 2019.
- Cruz Nunes, F., Delunel, R., Schlunegger, F., Akçar, N., and Kubik, P. W.: Bedrock bedding, landsliding and erosional budgets in the Central European Alps, *Terra Nova*, 27, 370–378, <https://doi.org/10.1111/ter.12169>, 2015.
- Da Silva Guimarães, E., Delunel, R., Schlunegger, F., Akçar, N., Stutenbecker, L., and Christl, M.: Cosmogenic and Geological Evidence for the Occurrence of a Ma-Long Feedback between Uplift and Denudation, Chur Region, Swiss
775 Alps, *Geosciences*, 11, 339, <https://doi.org/10.3390/geosciences11080339>, 2021.
- Delunel, R., Schlunegger, F., Valla, P. G., Dixon, J., Glotzbach, C., Hippe, K., Kober, F., Molliex, S., Norton, K. P., Salcher, B., Wittmann, H., Akçar, N., and Christl, M.: Late-Pleistocene catchment-wide denudation patterns across the European Alps, *Earth-Science Reviews*, 211, 103407, <https://doi.org/10.1016/j.earscirev.2020.103407>, 2020.
- Delunel, R., Bourlès, D. L., van der Beek, P. A., Schlunegger, F., Leya, I., Masarik, J., and Paquet, E.: Snow shielding
780 factors for cosmogenic nuclide dating inferred from long-term neutron detector monitoring, *Quaternary Geochronology*, 24, 16–26, <https://doi.org/10.1016/j.quageo.2014.07.003>, 2014.
- [Delunel, R., van der Beek, P. A., Carcaillet, J., Bourlès, D. L., and Valla, P. G.: Frost-cracking control on catchment denudation rates: Insights from in situ produced 10Be concentrations in stream sediments \(Ecrins–Pelvoux massif, French Western Alps\), *Earth and Planetary Science Letters*, 293, 72–83, <https://doi.org/10.1016/j.epsl.2010.02.020>,
785 2010.](#)
- DiBiase, R. A.: Short communication: Increasing vertical attenuation length of cosmogenic nuclide production on steep slopes negates topographic shielding corrections for catchment erosion rates, *Earth Surf. Dynam.*, 6, 923–931, <https://doi.org/10.5194/esurf-6-923-2018>, 2018.
- DiBiase, R. A., Neely, A. B., Whipple, K. X., Heimsath, A. M., and Niemi, N. A.: Hillslope Morphology Drives Variability
790 of Detrital 10 Be Erosion Rates in Steep Landscapes, *Geophysical Research Letters*, 50, <https://doi.org/10.1029/2023GL104392>, 2023.

- DiBiase, R. A., Whipple, K. X., Heimsath, A. M., and Ouimet, W. B.: Landscape form and millennial erosion rates in the San Gabriel Mountains, CA, *Earth and Planetary Science Letters*, 289, 134–144, <https://doi.org/10.1016/j.epsl.2009.10.036>, 2010.
- 795 Diem, B.: Die Untere Meeresmolasse zwischen der Saane (Westschweiz) und der Ammer (Oberbayern)., *Exlogae Geol. Helv.*, 493–559, 1986.
- Dingle, E. H., Sinclair, H. D., Attal, M., Rodés, Á., and Singh, V.: Temporal variability in detrital ¹⁰Be concentrations in a large Himalayan catchment, *Earth Surf. Dynam.*, 6, 611–635, <https://doi.org/10.5194/esurf-6-611-2018>, 2018.
- do Prado, A. H., Mair, D., Garefalakis, P., Schmidt, C., Whittaker, A., Castellort, S., and Schlunegger, F.: Check dam impact on sediment loads: example of the Guerbe River in the Swiss Alps – a catchment scale experiment, *Hydrol. Earth Syst. Sci.*, 28, 1173–1190, <https://doi.org/10.5194/hess-28-1173-2024>, 2024.
- 800 Frei, P., Kotlarski, S., Liniger, M. A., and Schär, C.: Future snowfall in the Alps: projections based on the EURO-CORDEX regional climate models, *The Cryosphere*, 12, 1–24, <https://doi.org/10.5194/tc-12-1-2018>, 2018.
- Glaus, G., Delunel, R., Stutenbecker, L., Akçar, N., Christl, M., and Schlunegger, F.: Differential erosion and sediment fluxes in the Landquart basin and possible relationships to lithology and tectonic controls, *Swiss J Geosci*, 112, 453–473, <https://doi.org/10.1007/s00015-019-00344-3>, 2019.
- 805 Granger, D. E., Kirchner, J. W., and Finkel, R.: Spatially Averaged Long-Term Erosion Rates Measured from in Situ-Produced Cosmogenic Nuclides in Alluvial Sediment, *The Journal of Geology*, 104, 249–257, <https://doi.org/10.1086/629823>, 1996.
- 810 Haldimann, P., Graf, H. R., Jost, J., and Kälin, D. (Eds.): 1071 Bülach, *Geologischer Atlas der Schweiz*, 151 = Blatt 1071, Bundesamt für Landestopografie swisstopo Geologische Landesaufnahme, Wabern, 2017.
- Halsted, C., Bierman, P., Codilean, A., Corbett, L., and Caffee, M.: Global analysis of in situ cosmogenic ²⁶Al/ ¹⁰Be ratios in fluvial sediments indicates widespread sediment storage and burial during transport, <https://doi.org/10.5194/gchron-2024-22>, 2024.
- 815 Heinz, R. A., Blau, R. V., Nicol, G., and Burkhalter, R.: Thun, *Geologischer Atlas der Schweiz* 1, 177 = Blatt 1207, Bundesamt für Landestopografie swisstopo, Wabern, 2023.
- Hippe, K., Kober, F., Wacker, L., Fahrni, S. M., Ivy-Ochs, S., Akçar, N., Schlüchter, C., and Wieler, R.: An update on in situ cosmogenic ¹⁴C analysis at ETH Zürich, *Nuclear Instruments and Methods in Physics Research Section B: Beam Interactions with Materials and Atoms*, 294, 81–86, <https://doi.org/10.1016/j.nimb.2012.06.020>, 2013.
- 820 Hippe, K.: Constraining processes of landscape change with combined in situ cosmogenic ¹⁴C-¹⁰Be analysis, *Quaternary Science Reviews*, 173, 1–19, <https://doi.org/10.1016/j.quascirev.2017.07.020>, 2017.
- Hippe, K. and Lifton, N. A.: Calculating Isotope Ratios and Nuclide Concentrations for In Situ Cosmogenic ¹⁴C Analyses, *Radiocarbon*, 56, 1167–1174, <https://doi.org/10.2458/56.17917>, 2014.

- 825 Hippe, K., Gordijn, T., Picotti, V., Hajdas, I., Jansen, J. D., Christl, M., Vockenhuber, C., Maden, C., Akçar, N., and Ivy-Ochs, S.: Fluvial dynamics and ^{14}C - ^{10}Be disequilibrium on the Bolivian Altiplano, *Earth Surf. Process. Landforms*, 44, 766–780, <https://doi.org/10.1002/esp.4529>, 2019.
- Hippe, K., Kober, F., Zeilinger, G., Ivy-Ochs, S., Maden, C., Wacker, L., Kubik, P. W., and Wieler, R.: Quantifying denudation rates and sediment storage on the eastern Altiplano, Bolivia, using cosmogenic ^{10}Be , ^{26}Al , and in situ ^{14}C , *Geomorphology*, 179, 58–70, <https://doi.org/10.1016/j.geomorph.2012.07.031>, 2012.
- 830 Ivy-Ochs, S., Monegato, G., and Reitner, J. M.: The Alps: glacial landforms from the Last Glacial Maximum, 449–460, <https://doi.org/10.1016/B978-0-12-823498-3.00030-3>, 2022.
- Ivy-Ochs, S., Kerschner, H., Maisch, M., Christl, M., Kubik, P. W., and Schlüchter, C.: Latest Pleistocene and Holocene glacier variations in the European Alps, *Quaternary Science Reviews*, 28, 2137–2149, <https://doi.org/10.1016/j.quascirev.2009.03.009>, 2009.
- 835 Jäckle, S.: *Hydrologischer atlas der Schweiz. Wildbach Gürbe Gurnigel – Wattenwil*, Vol. 6.1, Bern, Switzerland, Bern, available at: <https://hydrologischeratlas.ch/produkte/exkursionen/bern/61>, last access: March 2024, 2013.
- Jautzy, T., Rixhon, G., Braucher, R., Delunel, R., Valla, P. G., Schmitt, L., and Team, A.: Cosmogenic (un-)steadiness revealed by paired-nuclide catchment-wide denudation rates in the formerly half-glaciated Vosges Mountains (NE France), *Earth and Planetary Science Letters*, 625, 118490, <https://doi.org/10.1016/j.epsl.2023.118490>, 2024.
- 840 Jonas, T., Marty, C., and Magnusson, J.: Estimating the snow water equivalent from snow depth measurements in the Swiss Alps, *Journal of Hydrology*, 378, 161–167, <https://doi.org/10.1016/j.jhydrol.2009.09.021>, 2009.
- Knudsen, M. F., Nørgaard, J., Grischott, R., Kober, F., Egholm, D. L., Hansen, T. M., and Jansen, J. D.: New cosmogenic nuclide burial-dating model indicates onset of major glaciations in the Alps during Middle Pleistocene Transition, *Earth and Planetary Science Letters*, 549, 116491, <https://doi.org/10.1016/j.epsl.2020.116491>, 2020.
- 845 Kober, F., Hippe, K., Salcher, B., Ivy-Ochs, S., Kubik, P. W., Wacker, L., and Hählen, N.: Debris-flow-dependent variation of cosmogenically derived catchment-wide denudation rates, *Geology*, 2012, 935–938, 2012.
- Kubik, P. W. and Christl, M.: ^{10}Be and ^{26}Al measurements at the Zurich 6MV Tandem AMS facility, *Nuclear Instruments and Methods in Physics Research Section B: Beam Interactions with Materials and Atoms*, 268, 880–883, <https://doi.org/10.1016/j.nimb.2009.10.054>, 2010.
- 850 Lal, D.: Cosmic ray labeling of erosion surfaces: in situ nuclide production rates and erosion models, *Earth and Planetary Science Letters*, 104, 424–439, [https://doi.org/10.1016/0012-821X\(91\)90220-C](https://doi.org/10.1016/0012-821X(91)90220-C), 1991.
- Latif, I.: *Denudation Rates, Sediment Supply and Grain Size Pattern in an Anthropogenically Influenced Torrent, Central Alps, Switzerland.*, Unpublished Ms thesis, Institute of Geological Sciences, University of Bern, Bern, 2019.
- Lupker, M., Hippe, K., Wacker, L., Steinemann, O., Tikhomirov, D., Maden, C., Haghypour, N., and Synal, H.-A.: In-situ cosmogenic ^{14}C analysis at ETH Zürich: Characterization and performance of a new extraction system, *Nuclear Instruments and Methods in Physics Research Section B: Beam Interactions with Materials and Atoms*, 457, 30–36, <https://doi.org/10.1016/j.nimb.2019.07.028>, 2019.

- Marc, O., Behling, R., Andermann, C., Turowski, J. M., Illien, L., Roessner, S., and Hovius, N.: Long-term erosion of the Nepal Himalayas by bedrock landsliding: the role of monsoons, earthquakes and giant landslides, *Earth Surf. Dynam.*, 7, 107–128, <https://doi.org/10.5194/esurf-7-107-2019>, 2019.
- 860
- Maxeiner, S., Synal, H.-A., Christl, M., Suter, M., Müller, A., and Vockenhuber, C.: Proof-of-principle of a compact 300 kV multi-isotope AMS facility, *Nuclear Instruments and Methods in Physics Research Section B: Beam Interactions with Materials and Atoms*, 439, 84–89, <https://doi.org/10.1016/j.nimb.2018.11.028>, 2019.
- [Mudd, S. M.: Detection of transience in eroding landscapes, *Earth Surf. Process. Landforms*, 42, 24–41, <https://doi.org/10.1002/esp.3923>, 2017.](https://doi.org/10.1002/esp.3923)
- 865
- NGKAT: Naturgefahrenkataster, Amt für Wald und Naturgefahren des Kantons Bern, <https://www.agi.dij.be.ch/de/start/geoportal/geodaten/detail.html?type=geoproduct&code=NGKAT>, last access: 2024, 2024.
- Niemi, N. A., Oskin, M., Burbank, D. W., Heimsath, A. M., and Gabet, E. J.: Effects of bedrock landslides on cosmogenically determined erosion rates, *Earth and Planetary Science Letters*, 237, 480–498, <https://doi.org/10.1016/j.epsl.2005.07.009>, 2005.
- 870
- Nishiizumi, K., Winterer, E. L., Kohl, C. P., Klein, J., Middleton, R., Lal, D., and Arnold, J. R.: Cosmic ray production rates of 10 Be and 26 Al in quartz from glacially polished rocks, *J. Geophys. Res.*, 94, 17907–17915, <https://doi.org/10.1029/JB094iB12p17907>, 1989.
- 875
- Norton, K. P., Abbühl, L. M., and Schlunegger, F.: Glacial conditioning as an erosional driving force in the Central Alps, *Geology*, 38, 655–658, <https://doi.org/10.1130/G31102.1>, 2010.
- Pedregosa, F., Varoquaux, G., Gramfort, A., Michel, V., Thirion, B., Grisel, O., Blondel, M., Prettenhofer, P., Weiss, R., Dubourg, V., Vanderblat, J., Passos, A., and Cournapeau, D.: Scikit-learn: Machine Learning in Python, *Journal of Machine Learning Research*, 2825–2830, 2011.
- 880
- Ramirez, J. A., Mertin, M., Peleg, N., Horton, P., Skinner, C., Zimmermann, M., and Keiler, M.: Modelling the long-term geomorphic response to check dam failures in an alpine channel with CAESAR-Lisflood, *International Journal of Sediment Research*, 37, 687–700, <https://doi.org/10.1016/j.ijsrc.2022.04.005>, 2022.
- Reber, R., Delunel, R., Schlunegger, F., Litty, C., Madella, A., Akçar, N., and Christl, M.: Environmental controls on 10 Be-based catchment-averaged denudation rates along the western margin of the Peruvian Andes, *Terra Nova*, 29, 282–293, <https://doi.org/10.1111/ter.12274>, 2017.
- 885
- Riley, S. J., DeGloria, S., and Elliot, R.: A Terrain Ruggedness Index that Quantifies Topographic Heterogeneity, *Intermountain Journal of Sciences*, 23–27, 1999.
- Roda-Boluda, D. C., D'Arcy, M., Whittaker, A. C., Gheorghiu, D. M., and Rodés, Á.: 10Be erosion rates controlled by transient response to normal faulting through incision and landsliding, *Earth and Planetary Science Letters*, 507, 140–153, <https://doi.org/10.1016/j.epsl.2018.11.032>, 2019.
- 890

- Salvisberg, M.: Taming the torrent: changes in flood protection at the Gürbe River (Switzerland) from the nineteenth century until today, *Water history*, 14, 355–377, <https://doi.org/10.1007/s12685-022-00312-z>, 2022.
- Salvisberg, M.: Der Hochwasserschutz an der Gürbe: Eine Herausforderung für Generationen (1855-2010), *Wirtschafts-, Sozial- und Umweltgeschichte (WSU)*, Band 7, Schwabe Verlag, Basel, 406 pp., 2017.
- 895 Savi, S., Delunel, R., and Schlunegger, F.: Efficiency of frost-cracking processes through space and time: An example from the eastern Italian Alps, *Geomorphology*, 232, 248–260, <https://doi.org/10.1016/j.geomorph.2015.01.009>, 2015.
- Savi, S., Norton, K., Picotti, V., Brardinoni, F., Akçar, N., Kubik, P. W., Delunel, R., and Schlunegger, F.: Effects of sediment mixing on ^{10}Be concentrations in the Zielbach catchment, central-eastern Italian Alps, *Quaternary Geochronology*, 19, 148–162, <https://doi.org/10.1016/j.quageo.2013.01.006>, 2014.
- 900 Schlunegger, F. and Garefalakis, P.: Einführung in die Sedimentologie, Schweitzerbart, Stuttgart, 305 pp., 2023.
- Schlunegger, F. and Norton, K. P.: Water versus ice: The competing roles of modern climate and Pleistocene glacial erosion in the Central Alps of Switzerland, *Tectonophysics*, 602, 370–381, <https://doi.org/10.1016/j.tecto.2013.03.027>, 2013.
- Schwanghart, W. and Scherler, D.: Short Communication: TopoToolbox 2 – MATLAB-based software for topographic analysis and modeling in Earth surface sciences, *Earth Surf. Dynam.*, 2, 1–7, <https://doi.org/10.5194/esurf-2-1-2014>, 2014.
- 905 [Sibson, R.: A Brief Description of Natural Neighbor Interpolation, in: Interpolating Multivariate Data, John Wiley & Sons, New York, 21–36, 1981.](#)
- Simpson, G. and Schlunegger, F.: Topographic evolution and morphology of surfaces evolving in response to coupled fluvial and hillslope sediment transport, *J. Geophys. Res.*, 108, <https://doi.org/10.1029/2002JB002162>, 2003.
- 910 Skov, D. S., Egholm, D. L., Jansen, J. D., Sandiford, M., and Knudsen, M. F.: Detecting landscape transience with in situ cosmogenic ^{14}C and ^{10}Be , *Quaternary Geochronology*, 54, 101008, <https://doi.org/10.1016/j.quageo.2019.101008>, 2019.
- Slosson, J. R., Hoke, G. D., and Lifton, N.: Non-Steady-State ^{14}C - ^{10}Be and Transient Hillslope Dynamics in Steep High Mountain Catchments, *Geophysical Research Letters*, 49, <https://doi.org/10.1029/2022GL100365>, 2022.
- 915 [Starke, J., Ehlers, T. A., and Schaller, M.: Latitudinal effect of vegetation on erosion rates identified along western South America, *Science \(New York, N.Y.\)*, 367, 1358–1361, <https://doi.org/10.1126/science.aaz0840>, 2020.](#)
- Stone, J. O.: Air pressure and cosmogenic isotope production, *J. Geophys. Res.*, 105, 23753–23759, <https://doi.org/10.1029/2000JB900181>, 2000.
- Stutenbecker, L., Delunel, R., Schlunegger, F., Silva, T. A., Šegvić, B., Girardclos, S., Bakker, M., Costa, A., Lane, S. N., Loizeau, J.-L., Molnar, P., Akçar, N., and Christl, M.: Reduced sediment supply in a fast eroding landscape? A multi-proxy sediment budget of the upper Rhône basin, Central Alps, *Sedimentary Geology*, 375, 105–119, <https://doi.org/10.1016/j.sedgeo.2017.12.013>, 2018.
- Swisstopo: GeoCover, Federal Office of Topography swisstopo, <https://www.swisstopo.admin.ch/en/geological-model-2d-geocover#GeoCover---Download>, last access: 2024, 2024a.

- 925 Swisstopo: GeoMaps 500 Pixel, Federal Office of Topography swisstopo, <https://www.swisstopo.admin.ch/en/geomaps-500-pixel>, last access: 2024, 2024b.
- Swisstopo: Swiss Map Raster 10, Federal Office of Topography swisstopo, <https://www.swisstopo.admin.ch/de/landeskarte-swiss-map-raster-10>, last access: 2024, 2024c.
- Swisstopo: swissALTI3D, Federal Office of Topography swisstopo, <https://www.swisstopo.admin.ch/en/height-model-swissalti3d>, last access: 2024, 2024d.
- 930 Swisstopo: SWISSIMAGE 10 cm, Federal Office of Topography swisstopo, <https://www.swisstopo.admin.ch/de/orthobilder-swissimage-10-cm>, last access: 2024, 2024e.
- Swisstopo: SWISSIMAGE HIST, Federal Office of Topography swisstopo, <https://www.swisstopo.admin.ch/en/orthoimage-swissimage-hist>, last access: 2024, 2024f.
- 935 Synal, H.-A., Stocker, M., and Suter, M.: MICADAS: A new compact radiocarbon AMS system, *Nuclear Instruments and Methods in Physics Research Section B: Beam Interactions with Materials and Atoms*, 259, 7–13, <https://doi.org/10.1016/j.nimb.2007.01.138>, 2007.
- Tercier, P. J. and Bieri, P.: Gurnigel (AS 348 - 351, Guggisberg - Rüscheegg - Plasselb - Gantrisch)., Sans notice explicative (Feuille entoilée, pliée), 1961.
- 940 Tucker, G. E. and Slingerland, R.: Drainage basin responses to climate change, *Water Resour. Res.*, 33, 2031–2047, <https://doi.org/10.1029/97WR00409>, 1997.
- van den Berg, F., Schlunegger, F., Akçar, N., and Kubik, P.: 10 Be-derived assessment of accelerated erosion in a glacially conditioned inner gorge, Entlebuch, Central Alps of Switzerland, *Earth Surf. Process. Landforms*, 37, 1176–1188, <https://doi.org/10.1002/esp.3237>, 2012.
- 945 Vanacker, V., Blanckenburg, F. von, Govers, G., Molina, A., Campforts, B., and Kubik, P. W.: Transient river response, captured by channel steepness and its concavity, *Geomorphology*, 228, 234–243, <https://doi.org/10.1016/j.geomorph.2014.09.013>, 2015.
- vonBlanckenburg, F.: The control mechanisms of erosion and weathering at basin scale from cosmogenic nuclides in river sediment, *Earth and Planetary Science Letters*, 237, 462–479, <https://doi.org/10.1016/j.epsl.2005.06.030>, 2005.
- 950 West, A. J., Hetzel, R., Li, G., Jin, Z., Zhang, F., Hilton, R. G., and Densmore, A. L.: Dilution of ¹⁰Be in detrital quartz by earthquake-induced landslides: Implications for determining denudation rates and potential to provide insights into landslide sediment dynamics, *Earth and Planetary Science Letters*, 396, 143–153, <https://doi.org/10.1016/j.epsl.2014.03.058>, 2014.
- Winkler, W.: Palaeocurrents and petrography of the Gurnigel-Schlieren flysch: A basin analysis, *Sedimentary Geology*, 40, 169–189, [https://doi.org/10.1016/0037-0738\(84\)90045-9](https://doi.org/10.1016/0037-0738(84)90045-9), 1984.
- 955 Wittmann, H. and vonBlanckenburg, F.: Cosmogenic nuclide budgeting of floodplain sediment transfer, *Geomorphology*, 109, 246–256, <https://doi.org/10.1016/j.geomorph.2009.03.006>, 2009.

- Wittmann, H., Oelze, M., Gaillardet, J., Garzanti, E., and Blanckenburg, F. von: A global rate of denudation from cosmogenic nuclides in the Earth's largest rivers, *Earth-Science Reviews*, 204, 103147, 960 <https://doi.org/10.1016/j.earscirev.2020.103147>, 2020.
- Wittmann, H., Blanckenburg, F. von, Maurice, L., Guyot, J. L., and Kubik, P. W.: Recycling of Amazon floodplain sediment quantified by cosmogenic ^{26}Al and ^{10}Be , *Geology*, 39, 467–470, <https://doi.org/10.1130/G31829.1>, 2011.
- Wittmann, H., vonBlanckenburg, F., Guyot, J. L., Maurice, L., and Kubik, P. W.: From source to sink: Preserving the cosmogenic ^{10}Be -derived denudation rate signal of the Bolivian Andes in sediment of the Beni and Mamoré foreland 965 basins, *Earth and Planetary Science Letters*, 288, 463–474, <https://doi.org/10.1016/j.epsl.2009.10.008>, 2009.
- Yanites, B. J., Tucker, G. E., and Anderson, R. S.: Numerical and analytical models of cosmogenic radionuclide dynamics in landslide-dominated drainage basins, *J. Geophys. Res.*, 114, <https://doi.org/10.1029/2008JF001088>, 2009.
- Zimmermann, M., Perren, B., and Fehr, S.: *Verbau Gürbe im Gebirge, Erneuerung und Unterhalt: Überprüfung der Wirksamkeit und der Wirtschaftlichkeit*, IMPULS AG and NDR Consulting GmbH, Thun, 2016. 970